塑膠管固化分析
Solidifying Plastic Pipe

A. M. Schmalzer, A. M. Mertz, D. N. Githuku, A. J. Giacomin*

摘要

擠出製程中為了讓剛擠製出環形鋼模的塑膠管件從高溫高黏度之熔融態固化至一般成品。一般而言，其冷卻方法可為將高溫成品擠製進入冷卻水中或者噴灑冷卻水至產品表面，稱之為淬火。此方式為控制管件外壁溫度等於冷卻水的溫度。本文首先針對此階段等溫管件外壁的條件下，提出一精確的塑膠管淬火相變化解析解，再進行固化時間對溫度及半徑的方程式之無因次化。同時檢驗其冷卻未完全之情況。最後藉由比對有限元素解來提升此解析解之正確性，同時搭配案例驗證以幫助工程師設計淬火冷卻槽。

關鍵詞：塑膠管，塑膠管固化，紐曼問題，史蒂芬問題，相變化熱傳，凝固，淬火冷卻槽設計，管件淬火槽，塑膠管冷卻

Abstract

When plastic pipe is extruded, it emerges from an annular die as hot molten plastic. This highly viscous liquid must then be solidified. This is normally accomplished by either plunging it under cold water, or by spraying cold water onto its outer surface. Called *quenching*, this unit operation then solidifies the plastic by maintaining its outer wall temperature at the cold-water temperature. We first provide an exact analytical solution for the quenching of plastic pipe with phase change, subject to this cold, wet isothermal outer wall. We give the dimensionless solidification time as a function of the dimensionless solidification temperature and dimensionless radius. We then examine the case where the cooling is imperfect. Finally, we evaluate these analytical solutions by comparing them with their corresponding finite element solutions, and we then use these finite element solutions to delimit the accuracy of our analytical solutions. We include worked examples to help plastics engineers design the quench tank.

Keywords: plastic pipe, plastic pipe solidification, Neumann problem, Stefan problem, heat transfer with phase change, freezing, quench tank design, pipe quench tank, plastic pipe cooling

I. INTRODUCTION

In plastic pipe manufacturing, it is important to determine how long it will take for molten extrudate to solidify. The solidification rate of extrudate governs not only the quench tank length, but also the wall thickness distribution by delimiting how much sag occurs to the molten interior of the pipe. The goal of this paper is to help a plastics processing engineer define the required attributes of the quench tank based on the dimensionless cooling time of the extrudate.

By *quench tank* we mean a cooling chamber that either submerges the hot extrudate in cold water, or exposes it to a cold water spray. Though the inside of the pipe can also be spray cooled (called *internal cooling*), this is not normally done. This paper thus focuses on the case of *external cooling* with the adiabatic inner wall.

Solidification freezes residual stresses into the solidified pipe [1, 2] but, according to Doshi's iterative method for this problem [1], these residual stresses do not depend on the cooling rate (compare with *Fig. 3* through *Fig. 5* and *Fig. 8* of [3]).

Table 1 classifies the literature on the solidification of plastic pipe. For crystallizable polymers there is a change in enthalpy for the liquid-solid phase change at the solid-liquid interface of the solidifying extrudate. In this paper, we specifically ignore the kinetics of crystallization, which have been capably handled by Hansen and Wu [4] and Wu [5]. These kinetics govern the detailed microstructure of a solidifying crystallizable polymer. Though they affect important morphological details like the crystallinity, crystal

威斯康辛大學機械工程學系暨流變學中心
*Corresponding author. E-mail: giacomin@wisc.edu
Rheology Research Center and Mechanical Engineering Department, University of Wisconsin-Madison, Madison, WI 53706-1572
Manuscript received 19 March 2012; revised 1 May 2012; accepted 18 May 2012

Table 1 Pipe solidification literature

	Residual Stress	Crystallization Kinetics	Shrinkage	ΔH	Sag	Wall Boundary Condition	Method for Cooling	Reference
Kamp, *et al.* (1980)						$h_o, \mathscr{A}_i$	AA	[23]
Spivey and Barona (1980)						h_o, T_i	FD	[24]
Gebler and Racké (1982)	σ		$\Delta\rho$					[2]
Barnes (1989)						h_o, T_i	FDM	[25]
Wu (1990)		χ		ΔH		$\mathscr{A}_i$	FE	[5]
Hansen and Wu (1991)		χ		ΔH		$h_o, \mathscr{A}_i$	FE	[4]
Githuku (1992)				ΔH	CIP	$T_o, \mathscr{A}_i$	SE	[7]
Githuku and Giacomin (1992)					CIP			[8]
Githuku and Giacomin (1992)				ΔH	SE	$T_o, \mathscr{A}_i$ $h_o, \mathscr{A}_i$	SE	[9]
Githuku and Giacomin (1992)					CIP	$T_o, \mathscr{A}_i$	SE	[10]
Githuku and Giacomin (1993)					SE	$T_o, \mathscr{A}_i$	SE	[11]
Pittman, *et al.* (1994)			$\Delta\rho$			$h_o, \mathscr{A}_i$	FE	[26]
Pittman and Farah (1996)	σ	χ	$\Delta\rho$		FE	h_o, h_i	FE	[27]
This paper			$\Delta\rho$	ΔH		$T_o, \mathscr{A}_i$ $h_o, \mathscr{A}_i$	FE	
This paper			$\Delta\rho$	ΔH		$T_o, \mathscr{A}_i$ $h_o, \mathscr{A}_i$	A	

Legend: $\mathscr{A}_i \equiv$ Adiabatic inner wall; $\mathrm{A} \equiv$ Analytical; $\mathrm{AA} \equiv$ Approximate analytical; $\mathrm{CIP} \equiv$ Cascade of inclined planes; $\chi \equiv$ Crystallization kinetics; $\mathrm{FD} \equiv$ Finite difference; $\mathrm{FE} \equiv$ Finite element; $h_i \equiv$ Non-isothermal inner wall; $h_o \equiv$ Non-isothermal outer wall; $\Delta\mathrm{H} \equiv$ Phase change; $\mathrm{SE} \equiv$ Spectral element; $\Delta\rho \equiv$ Shrinkage; $T_o \equiv$ Isothermal outer wall; $T_i \equiv$ Isothermal inner wall; $\sigma \equiv$ Residual stress

size, and crystal orientation, we do not expect them to affect the required quench tank length, which is the subject of this paper. In this paper, we present an exact dimensionless analytical solution derived from first principles with worked examples to help the plastics engineer to calculate the required quench tank length.

II. ENERGY EQUATION

For plastic pipe solidification, we solve the energy equation in Cartesian coordinates, subject to an adiabatic inside surface, and differing boundary conditions on the outside. For solidification by quenching we first use the isothermal outer wall, and then for imperfect cooling, we examine the more complicated non-isothermal outer wall. We begin with the energy equation in Cartesian coordinates (see Eq. B.8-1 in [6]):

$$\rho\hat{C}_p\left(\frac{\partial T}{\partial t}+v_x\frac{\partial T}{\partial x}+v_y\frac{\partial T}{\partial y}+v_z\frac{\partial T}{\partial z}\right) = -\left[\frac{\partial q_x}{\partial x}+\frac{\partial q_y}{\partial y}+\frac{\partial q_z}{\partial z}\right]-\left(\frac{\partial \ln\rho}{\partial \ln T}\right)_p\frac{Dp}{Dt}-(\tau:\nabla \mathrm{v}) \qquad (1)$$

Neglecting the gravitational flow (called sag [7-11]), $v_x = v_y = v_z = 0$, and so the viscous dissipation due to flow also vanishes, $(\tau:\nabla \mathrm{v}) = 0$. So pipe solidification is one dimensional, and thus $q_x = q_z = 0$. Since the density of the liquid hardly changes with temperature, we neglect the remaining flow work term on the right of Eq. (1). Applying Fourier's law of heat conduction, Eq. (1) then yields:

$$\frac{\partial T}{\partial t} = \alpha\frac{\partial^2 T}{\partial y^2} \qquad (2)$$

We then wrap our solutions, obtained in Cartesian coordinates, into cylindrical coordinates. For this wrapping, we replace the slab thickness with $(R_o - R_i)$, and the proximity to the inner wall with $(r - R_i)$. Fig. 1 and Fig. 2, along with Table 2, define the variables for the problem geometries, and Table 3 defines the corresponding dimensionless quantities. Since the wrapped slab occupies less area than its Cartesian counterpart, we correct for this decrease in mass with the density correction factor:

$$\xi \equiv \left[\frac{1}{2}(1+k)\right]^{-1} \qquad (3)$$

which expedites the cooling compared to a flat slab.

III. SOLIDIFYING PIPE WITH ISOTHERMAL WALL

For quenched cooling of a finite slab subject to an adiabatic inner wall, we solve Eq. (2) subject to (see Eq. (12.1-31) in [6]):

Table 2 Dimensional variables

Absolute temperature	T	T	>0
Absolute temperature, initial	T_1	T	>0
Absolute temperature, inside wall	T_i	T	>0
Absolute temperature, liquid	T_ℓ	T	>0
Absolute temperature, melting	T_m	T	>0
Absolute temperature, quench tank fluid away from the pipe	T_∞	T	>0
Absolute temperature, quenching fluid	T_o	T	>0
Absolute temperature, solid	T_s	T	>0
Heat transfer coefficient	h	$Mt^{-3}T^{-1}$	≥ 0
Latent heat of fusion	$\Delta\hat{H}_f$	ML^2t^{-2}	>0; exothermic <0; endothermic
Mass density, molten plastic	ρ_ℓ	ML^{-3}	>0
Mass density, solidified plastic	ρ_s	ML^{-3}	>0
Position, solid-liquid interface	$S(t)$	L	>0
Pressure jump	P	$ML^{-1}t^{-2}$	>0
Proximity to outer wall	x	L	>0
Proximity to the middle of the wall	y	L	$-b\leq y\leq b$
Radius	r	L	≥ 0
Radius, inner wall	R_i	L	>0
Radius, outer wall	R_o	L	>0
Specific heat of solid phase	$\hat{C}_{p,s}$	$ML^2t^{-2}T^{-1}$	>0
Speed, solid-liquid interface	v_s	Lt^{-1}	>0
Thermal conductivity, molten plastic	k_ℓ	$MLt^{-3}T^{-1}$	>0
Thermal conductivity, solidified plastic	k_s	$MLt^{-3}T^{-1}$	>0
Thermal diffusivity	α	L^2t^{-1}	>0
Thermal diffusivity, molten plastic	α_ℓ	L^2t^{-1}	>0
Thermal diffusivity, solidified plastic	α_s	L^2t^{-1}	>0
Time	t	t	>0
Wall half-thickness	b	L	>0

Legend: $M\equiv$ Mass; $L\equiv$ Length; $t\equiv$ Time; $T\equiv$ Temperature

$$T(r,0)=T_1 \tag{4}$$

$$T(R_0-R_i,t)=T_0 \tag{5}$$

$$\left.\frac{dT}{dy}\right|_{y=0}=T'(0,t)=0 \tag{6}$$

and then wrapping the solution into cylindrical coordinates and applying the curvature correction:

$$\frac{T-T_o}{T_1-T_o}=2\sum_{n=0}^{\infty}\frac{(-1)^n}{\left(n+\frac{1}{2}\right)\pi}\exp\left[-\left(n+\tfrac{1}{2}\right)^2\pi^2\xi\frac{\alpha_\ell t}{\left(R_o-R_i\right)^2}\right]\cos\left(n+\tfrac{1}{2}\right)\pi\left(\frac{r-R_i}{R_o-R_i}\right) \tag{7}$$

For a crystallizable polymer, where the thermal properties can differ across the solid-liquid interface, and where latent heat can be absorbed at the solid-liquid interface, and where the density can change at this same interface, and where the liquid pressure can jump at this interface, we include the thermal diffusivity factor $\Lambda\equiv(\lambda/\lambda_0)^2$:

$$\frac{T-T_o}{T_1-T_o}=2\sum_{n=0}^{\infty}\frac{(-1)^n}{\left(n+\frac{1}{2}\right)\pi}\exp\left[-\left(n+\tfrac{1}{2}\right)^2\pi^2\xi\frac{\Lambda\alpha_\ell t}{\left(R_o-R_i\right)^2}\right]\cos\left(n+\tfrac{1}{2}\right)\pi\left(\frac{r-R_i}{R_o-R_i}\right) \tag{8}$$

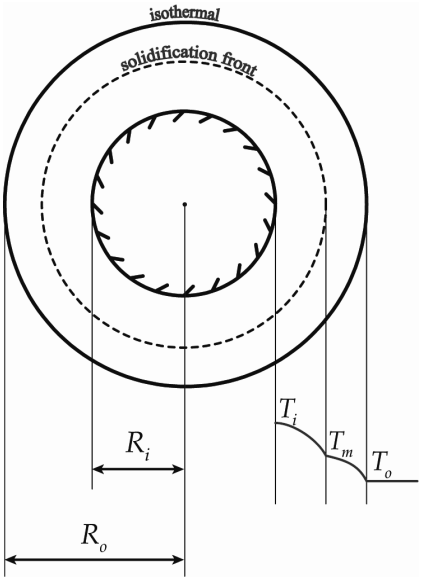

Fig. 1 Thermal boundary conditions for solidifying pipe with isothermal outer wall

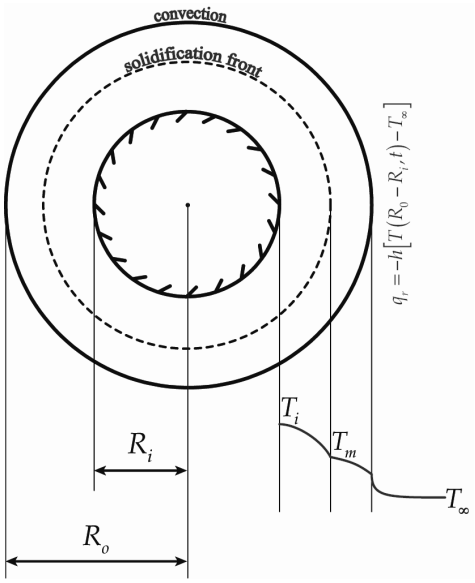

Fig. 2 Thermal boundary conditions for solidifying pipe with non-isothermal outer wall

Table 3 Dimensionless groups and variables

Biot number	$\mathrm{Bi} \equiv \frac{h}{k_s}\left(R_o - R_i\right)$	≥ 0
Cooling time	$\tau \equiv \frac{\alpha_\ell t}{\left(R_o - R_i\right)^2}$	≥ 0
Density correction factor	$\xi \equiv \left[\frac{1}{2}(1+k)\right]^{-1}$	$1 \leq \xi \leq 2$
Difference between the melting point and the extrudate temperature	$\Theta_m \equiv \frac{T_m - T_o}{T_1 - T_o}$	$0 \leq \Theta_m < 1$
Heat of fusion	$\mathbb{H} \equiv \frac{\Delta \hat{H}_f}{\hat{C}_{p,s}\left(T_i - T_o\right)}$	≥ 0
Pipe radius	$\mathscr{R} \equiv \frac{r - R_i}{R_o - R_i}$	$0 \leq \mathscr{R} \leq 1$
Pipe wall thickness ratio	$\kappa \equiv \frac{R_i}{R_o}$	$0 \leq \kappa \leq 1$
Solidification coefficient	λ	>0
Solidification coefficient for $\mathbb{H} = 0$	λ_0	>0
Temperature	$\Theta \equiv \frac{T(r,t) - T_0}{T_1 - T_0}$	$0 \leq \Theta \leq 1$
Temperature at the inside wall	$\Theta_i \equiv \frac{T_i - T_o}{T_1 - T_o}$	$0 \leq \Theta_i \leq 1$
Temperature, liquid phase	$\Theta_\ell \equiv \frac{T_\ell - T_o}{T_1 - T_o}$	$0 \leq \Theta_\ell \leq 1$
Temperature, solid phase	$\Theta_s \equiv \frac{T_s - T_o}{T_1 - T_o}$	$0 \leq \Theta_s \leq 1$
Thermal diffusivity factor	$\Lambda \equiv \left(\frac{\lambda}{\lambda_0}\right)^2$	>0

where λ is given by Eqs. (39)-(42) [as shown in APPENDIX A], which descend with the level of accuracy desired by (and amount of information available to) the engineer.

Adimensionalizing Eq. (8) yields:

$$\Theta\left(\mathscr{R}, \tau\right) = 2\sum_{n=0}^{\infty} \frac{(-1)^n}{\left(n+\frac{1}{2}\right)\pi} \exp\left[-\left(n+\tfrac{1}{2}\right)^2 \pi^2 \Lambda \xi \tau\right] \cos\left(n+\tfrac{1}{2}\right)\pi\mathscr{R} \quad (9)$$

where the dimensionless temperature, time and radial position, Θ, τ and $\mathscr{R}$, are defined in Table 3. For the design of plastic pipe solidification equipment, we are interested in the inside wall temperature $\left(\mathscr{R} = 0\right)$:

$$\Theta_i \equiv \Theta\left(0, \tau\right) = 2\sum_{n=0}^{\infty} \frac{(-1)^n}{\left(n+\frac{1}{2}\right)\pi} \exp\left[-\left(n+\tfrac{1}{2}\right)^2 \pi^2 \Lambda \xi \tau\right] \quad (10)$$

which is the main result of this paper. Eq. (10) is the basis for designing the cooling system for pipe manufacture, when the outer wall is quenched. Fig. 3 and Fig. 4 are plotted from Eq. (10), and can be used to determine the residence time required for solidifying the pipe, or to cool it to some prescribed temperature below the melting point T_m.

IV. SOLIDIFYING PIPE WITH NON-ISOTHERMAL WALL

For imperfect cooling of a finite slab subject to an adiabatic inner wall, we solve Eq. (2) subject to Eq. (4) and also to (see Chapter III, § 3.11 (i) of [12]):

$$q_y = -k_s \left.\frac{dT}{dy}\right|_{y=R_0-R_i} = -k_s T'\left(R_0 - R_i, t\right) = -h\left[T\left(R_0 - R_i, t\right) - T_\infty\right] \quad (11)$$

$$q_y\big|_{y=0} = -k_s \left.\frac{dT}{dy}\right|_{y=0} = -k_s T'\left(0, t\right) = 0 \quad (12)$$

and then wrapping the solution into cylindrical coordinates, applying the curvature correction ξ, including the thermal diffusivity factor Λ and adimensionalizing as in Section III above yields:

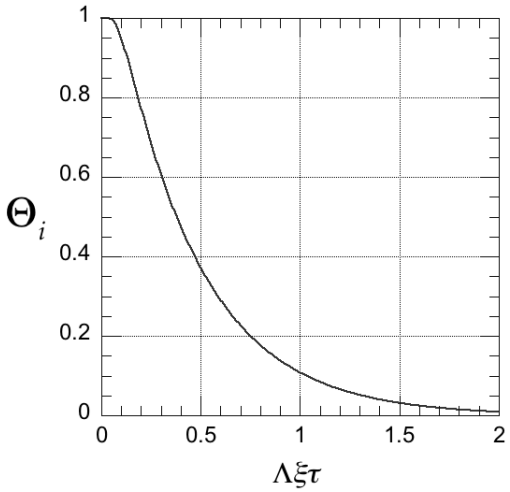

Fig. 3 Cooling of inside surface for isothermal outer wall [Eq. (10)]

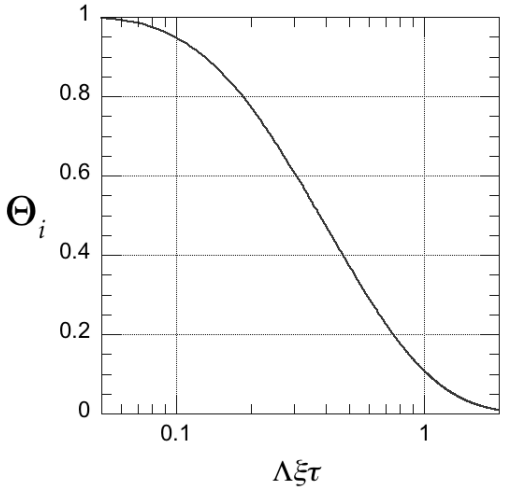

Fig. 4 Cooling of inside surface for isothermal outer wall (semi-log scale) [Eq. (10)]

$$\Theta = 2\sum_{n=1}^{\infty}\left\{\frac{\sec\beta_n}{1+\mathrm{Bi}+\frac{\beta_n^2}{\mathrm{Bi}}}\exp\left(-\beta_n\Lambda\xi\,\tau\right)\cos\left(\beta_n\mathscr{R}\right)\right\} \quad (13)$$

where $\beta_n, n=1,2,...$ are the positive real roots of:

$$\beta_n\tan\beta_n = \mathrm{Bi} \quad (14)$$

which can be read off of Fig. 5 and Fig. 6 (or found in Table 1 of App. IV of [12]) , and where:

$$\mathrm{Bi} \equiv \frac{h}{k_s}\left[R_o - R_i\right] \quad (15)$$

For the inside surface:

$$\Theta_i = 2\sum_{n=1}^{\infty}\left\{\frac{\sec\beta_n}{1+\mathrm{Bi}+\frac{\beta_n^2}{\mathrm{Bi}}}\exp\left(-\beta_n\Lambda\xi\tau\right)\right\} \quad (16)$$

and, at as $\tau\to\infty$, $\Theta_i\to 0$ as it should. Eq. (16), plotted in Fig. 7 and Fig. 8, is a main result of this paper.

V. FINITE ELEMENT SOLUTION

Finite element simulations of pipe cooling were conducted using the commercial software ANSYS POLYFLOW™ version 12.1 (ANSYS 2009a). This is an implementation of the numerical methods developed by Crochet and his team at Université Catholique de Louvain in Belgium [13]. A two dimensional planar (see Section 1.4.1 of [14]) two-fold symmetric (see Section 8.8 of [14]) representation was used for the cooling pipe. We solve the simplified equation of energy (see Eq. (13.1-1) in [14]; see also Table 1.1-1 Eq. C of [15] and §B.8 of [6]):

$$\frac{\partial}{\partial t}\rho\hat{U} = \rho\hat{C}_p\frac{DT}{Dt} = -\left(\nabla\cdot q\right) \quad (17)$$

Subject to an adiabatic boundary condition $\left(h=0\right)$ at the inner wall and then subject either to an isothermal outer wall (Fig. 9), or to a non-isothermal outer wall $\left(h>0\right)$ with a heat flux determined by Eq. (11) (Fig. 10). We used the 200-element quadrilateral mesh of Fig. 11 with refinement

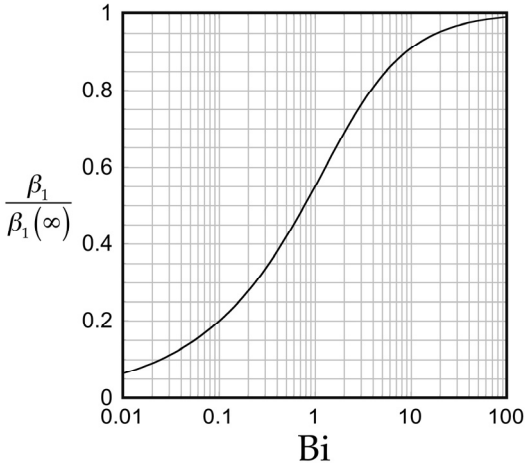

Fig. 5 Eq. (16) for determining β_1 where $\beta_1\left(\infty\right)=\pi/2$

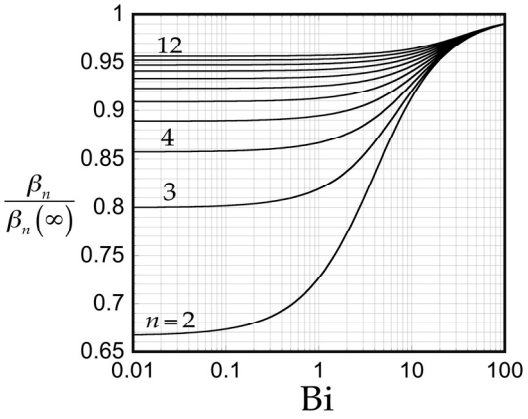

Fig. 6 Eq. (16) for determining β_n where $\beta_n(\infty)=\left[2(n-1)+1\right]\pi/2$

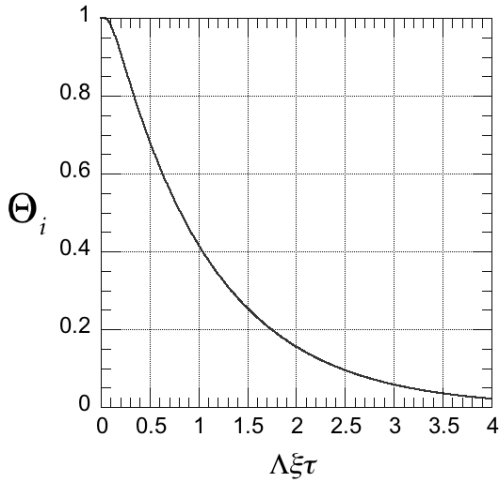

Fig. 7 Cooling of inside surface for non-isothermal outer wall, $\mathrm{Bi}=1$ [Eq. (16)]

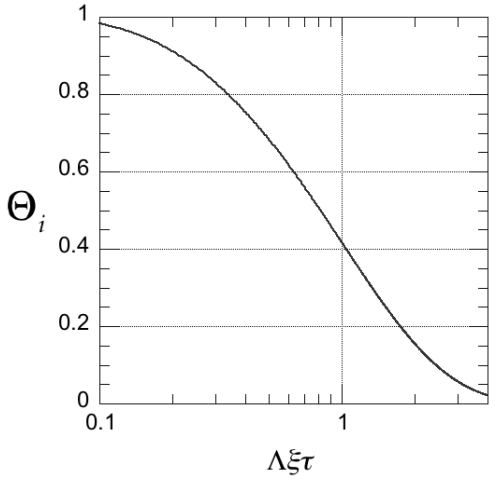

Fig. 8 Cooling of inside surface for non-isothermal outer wall, $\mathrm{Bi}=1$ (semi-log scale) [Eq. (16)]

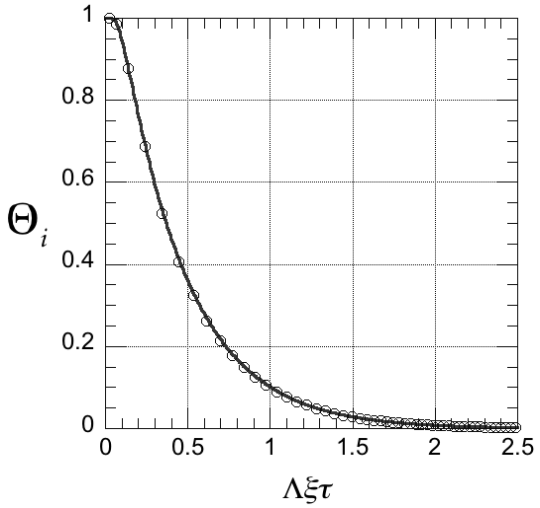

Fig. 9 Analytical solution (line) and finite element simulation (○) of cooling of inside surface for isothermal outer wall [Eq. (10)]

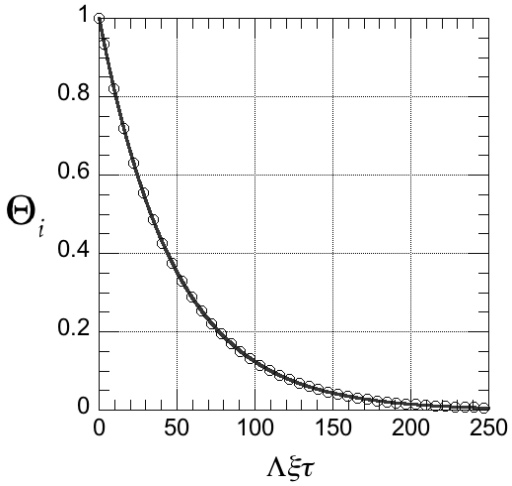

Fig. 10 Analytical solution (line) and finite element simulation (○) of inside surface for non-isothermal outer wall, $\mathrm{Bi}=1$

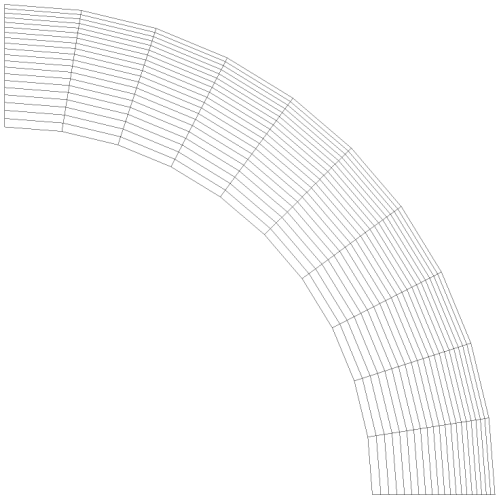

Fig. 11 Finite element mesh with 200 elements for quarter pipe

near the outer wall, generated using ANSYS Mesher™ [16]. The mesh is 20 elements wide in the radial direction, and 10 elements wide in the circumferential direction. The time-dependent integration method used for time stepping through the transient calculations is the Crank-Nicolson scheme given by Eq. (26.2-16) in [14]. Each isothermal outer wall calculation took roughly fifteen minutes, and the non-isothermal calculations, nearly 50 minutes, using just one core of a 64 bit 3.4 GHz quad core AMD processor (Advanced Micro Devices, Sunnyvale, CA).

VI. WORKED EXAMPLE: ISOTHERMAL OUTER WALL WITH PHASE CHANGE

Given the following process details for a high density polyethylene pipe cooling line [7, 8], $T_m=130°C$, $T_o=20°C$, $T_i=200°C$, $k_\ell=0.23\,\mathrm{W/mK}$, $k_s=0.31\,\mathrm{W/mK}$, $\alpha_\ell=1.10\times10^{-7}\,\mathrm{m^2/s}$, $\alpha_s=1.69\times10^{-7}\,\mathrm{m^2/s}$, $\Delta\hat{H}_f=1.365\times10^5\,J/kg$, $\rho=855\,\mathrm{kg/m^3}$, $\hat{C}_{p,s}=1926\,\mathrm{J/kgK}$, $R_o=0.4395\,\mathrm{m}$, and $R_i=0.3511\,\mathrm{m}$, determine the required residence time in the quench tank for the pipe to cool to the required exit temperature for solidification, T_m:

We first compute the dimensionless temperature of the inside wall required for solidification at the exit using the definition from Table 3:

$$\Theta_i=\frac{T_m-T_o}{T_i-T_o}=\frac{130-20}{200-20}=\frac{11}{18} \tag{18}$$

From this, we read $\Lambda\xi\tau=0.297$ from Fig. 4 at $\Theta_i=0.611$ [or we can also use Eq. (10)] from Table 3. For solidification of plastic pipe where crystallization occurs, we use Eq. (42) (or see Fig 12 and 13) to determine $\lambda=0.482$, and from Eq. (44) (or see Fig. 14) we determine $\lambda_0=0.621$. Therefore,

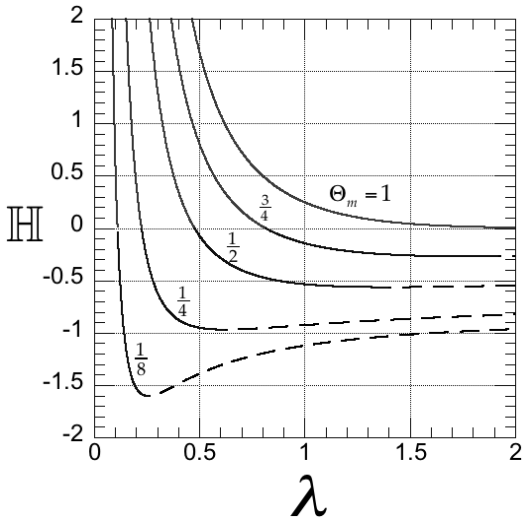

Fig. 12 Eq. (42) for $\Theta_m=\left[\frac{1}{8},\frac{1}{4},\frac{1}{2},\frac{3}{4},1\right]$ for exothermic $(H>0)$ and endothermic $(H<0)$ solidification

$$\Lambda = \left(\frac{\lambda}{\lambda_0}\right) = \left(\frac{0.482}{0.611}\right)^2 = 0.622 \tag{19}$$

Next we need to determine ξ using Eq. (3):

$$\xi = \tfrac{1}{2}\left(1+\kappa\right) = \tfrac{1}{2}\left(1+\frac{0.3511}{0.4395}\right) = 0.899 \tag{20}$$

Then solving τ for t:

$$t \equiv \frac{\tau}{\Lambda\xi\alpha_\ell}\left(R_o - R_i\right)^2$$
$$= \frac{0.297}{0.622(0.899)1.10\times10^{-7}\,\mathrm{m^2/s}}\left(0.4395\,\mathrm{m} - 0.3511\,\mathrm{m}\right)^2 = 10.5\,\mathrm{h} \tag{21}$$

which is the residence time required to solidify the plastic pipe.

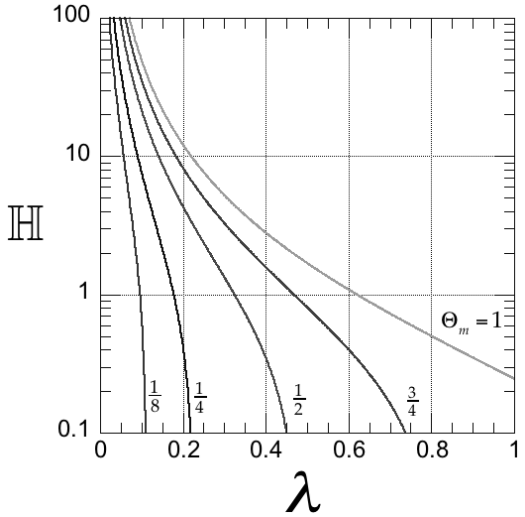

Fig. 13 Eq. (42) for $\Theta_m = \left[\tfrac{1}{8}, \tfrac{1}{4}, \tfrac{1}{2}, \tfrac{3}{4}, 1\right]$ for determining λ

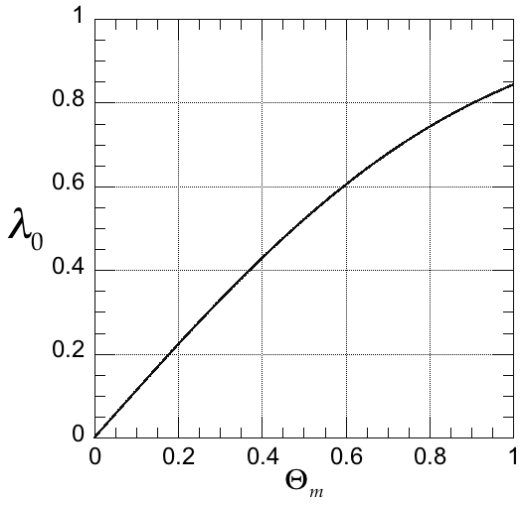

Fig. 14 Eq. (44) for determining λ_0

VII. WORKED EXAMPLE: ISOTHERMAL OUTER WALL WITHOUT PHASE CHANGE

If we neglect phase change, then $\Lambda = 1$, and using the same parameters from section VI the resulting time for cooling is:

$$t = \frac{\tau}{\Lambda\xi\alpha_\ell}\left(R_o - R_i\right)^2$$
$$= \frac{0.297}{1.00(0.899)1.10\times10^{-7}\,\mathrm{m^2/s}}\left(0.4395\,\mathrm{m} - 0.3511\,\mathrm{m}\right)^2 = 6.52\,\mathrm{h} \tag{22}$$

which is the required time to cool the pipe, neglecting phase change.

VIII. CONCLUSION

We solved the equation of energy to obtain exact analytical solutions for the solidification of plastic pipe for two outer-wall cooling configurations: isothermal and non-isothermal. We validate these solutions using finite element simulations. For the isothermal configuration, the main results of this paper are Eq. (10) and Fig. 4, and for the non-isothermal, Eq. (16) and Fig. 8. The working equations for designing solidification chambers for extruded plastic pipe are Eqs. (10) and (16).

These designs are governed by the dimensionless solidification coefficient, Λ, which depends upon every facet of the phase change interface. These facets include the melting temperature $\left(T_m\right)$, the latent heat of fusion $\left(\Delta\hat{H}_f\right)$, the changes in thermal properties $\left(\alpha_s, \alpha_\ell, \hat{C}_{p,s}, k_s, k_\ell\right)$, the shrinkage $\left(\rho_\ell/\rho_s\right)$, and the pressure jump $\left(P\right)$, each of which affects the solidification chamber design. Worked examples show plastics engineers how to use our results.

ACKNOWLEDGMENT

We are indebted to EDI, Inc. of Chippewa Falls, Wisconsin and Clearlam of Elk Grove Village, Il for their financial support. We are also greatly appreciative of Professor R. Byron Bird of the University of Wisconsin for helpful discussion on heat transfer with phase change. We are also greatly appreciative of Professor Chanyut Kolitawong, and Mr. Chaimongkol SaeNgow of King Mongkut's Institute of Technology North Bangkok for their help with proofreading this manuscript. We are also greatly appreciative of Mr. Adam W. Mix for his corrections. We thank Professor Jen-An Chang（張仁安） of the Mechanical Engineering Department of Chung Yuan University（中原大學）in Chungli City, Taiwan for translating the title and abstract into Chinese.

REFERENCES

[1] S. R. Doshi, "Prediction of residual stress distribution in plastic pipe extrusion," *Journal of Vinyl Technology*, vol. 11, no. 4, pp. 190-194, 1989.

[2] H. Gebler and H. H. Racké, "Determining internal stresses in thick walled plastic pipes," *Kunststoffe – German Plastics*, vol. 72, no. 1, pp. 33-38, 1982.

[3] R. K. Mittal and A. Khan, "Effect of various parameters on residual stresses in transparent polymeric tubes," *Intl. Polymer Processing*, vol. V, no. 2, pp. 142-148, 1990.
[4] M. G. Hansen and J. H. Wu, "Computer simulation of a crystallizing polymer in pipe extrusion," *49th Ann. Tech. Conf. ANTEC '91* (Montreal), pp. 2455-2460, 1991.
[5] J. H. Wu, "Computer simulation of steady-state pipe extrusion," PhD Thesis, The University of Tennessee, Mechanical Engineering Dept., Knoxville, TN, Aug. 1990.
[6] R. B. Bird, W. E. Stewart, and E. N. Lightfoot, *Transport Phenomena*, Revised 2nd Ed., Wiley & Sons, New York, 2007.
[7] D. N. Githuku, "Simulation of sag in plastic pipe extrusion," PhD Thesis, Texas A&M University, Mechanical Engineering Dept., College Station, TX, Feb. 1992.
[8] D. N. Githuku and A. J. Giacomin, "Simulation of slump in plastic pipe extrusion," *Journal of Engineering Materials and Technology*, vol. 114, no. 1, pp. 81-83, 1992.
[9] D. N. Githuku and A. J. Giacomin, "Heat transfer considerations in gravitational flows during plastic pipe extrusion," *Proc., 1st International Conference on Transport Phenomena in Processing*, Pacific Institute for Thermal Engineering, Honolulu, HI (March 22-26, 1992), S. I. Guceri, ed., Technomic Publishers Inc., Lancaster, PA, pp. 997-1012, 1992.
[10] D. N. Githuku and A. J. Giacomin, "Elimination of sag in plastic pipe," *Intl. Polymer Processing*, vol. VII, no. 2, pp. 140-143, 1992.
[11] D. N. Githuku and A. J. Giacomin, "A spectral element simulation of gravitational flow during plastic pipe extrusion," *Journal of Engineering Materials and Technology*, vol. 115, no. 4, pp. 433-439, 1993.
[12] H. S. Carslaw and J. C. Jaeger, *Conduction of Heat in Solids*, 2nd Ed., Oxford University Press, London, 1959.
[13] J. J. Van Schaftingen and M. J. Crochet, "A comparison of mixed methods for solving the flow of a Maxwell fluid," *Int. J. Numerical Methods Fluids*, vol. 4, pp. 1065-1081, 1984.
[14] "ANSYS POLYFLOW 12.1 User's Guide," ANSYS Inc., Canonsburg, PA, 2009.
[15] R. B. Bird, R. C. Armstrong, and O. Hassager, *Dynamics of Polymeric Liquids*, vol. 1, 2nd Ed., Wiley, New York, 1987.
[16] "ANSYS Meshing 12.1 User's Guide," ANSYS Inc., Canonsburg, PA, 2009.
[17] J. C. Slattery, *Momentum, Energy, and Mass Transfer in Continua*, 2nd Ed., Robert E. Krieger Publishing, New York, 1981.
[18] J. C. Slattery, *Solution manual for exercises in Momentum, Energy, and Mass Transfer in Continua*, 2nd Ed., Robert E. Krieger Publishing, Huntington, NY, 1981.
[19] N. W. Hale, Jr. and R. Viskanta, "Solid-liquid phase-change heat transfer and interface motion in materials cooled or heated from above or below," *Int. J. Heat Mass Transfer*, vol. 23, pp. 395-402, 1980.
[20] H. J. Janeschitz-Kriegl, *Crystallization Modalities in Polymer Melt Processing: Fundamental Aspects of Structure Formation*, Springer, Vienna, 2010.
[21] G. Eder and H. J. Janeschitz-Kriegl, "Stefan problem and polymer processing," *Polymer Bulletin*, vol. 11, pp. 93-98, 1984.
[22] G. Eder, H. J. Janeschitz-Kriegl, G. Krobath, and S. Liebauer, "Stefan problem and polymer processing," *Journal of Non-Newtonian Fluid Mech.*, vol. 23, pp. 107-122, 1986.
[23] W. Kamp and H. D. Kurz, "Cooling sections in polyolefin pipe extrusion," *Kunststoffe – German Plastics*, vol. 70, no. 5. pp. 8-12, 1980.
[24] J. J. Spivey and N. Barona, "Heat transfer in extrusion of plastic pipe downstream of the die," *ASME Journal of Heat Transfer*, pp. 1-5, 1980.
[25] C. M. Barnes, "An experimental and theoretical study of the cooling and solidification of thermoplastic polymers in various blow moulding and pipe extrusion situations," PhD Thesis, The University of Bradford, Dept. of Chemical Engineering, Bradford, U.K., 1989.
[26] J. F. T. Pittman, G. P. Whitham, S. Beech, and D. Gwynn, "Cooling and wall thickness uniformity in plastic pipe manufacture," *Intl. Polymer Processing*, vol. IX, no. 2, pp. 130-140, 1994.
[27] J. F. T. Pittman and I. A. Farah, "Comprehensive simulation of cooling process in plastic pipe manufacture," *Plastics, Rubber and Composites Processing and Applications*, vol. 25, no. 6, pp. 305-312, 1996.

APPENDIX A: OBTAINING λ

The quantity λ is given by a set of transcendental equations of descending level of accuracy [Eqs. (42), (41), (40), and (39)]. We derive each of these in this appendix. The engineer will select one of these based on the amount of property data available. Fig. 15 illustrates the moving boundary in a semi-infinite solid with the corresponding temperature profiles.

Using Table 3 to adimensionalize the temperature in Eq. (2), for the solid region, yields:

$$\frac{\partial \Theta_s}{\partial t} = \alpha_s \frac{\partial^2 \Theta_s}{\partial x^2} \tag{23}$$

but for the liquid region, we must now include a convective motion term (Eq. (2.33) from [7]):

$$\frac{\partial \Theta_\ell}{\partial t} + v_x \frac{\partial \Theta_\ell}{\partial x} = \alpha_\ell \frac{\partial^2 \Theta_\ell}{\partial x^2} \tag{24}$$

where v_x is the convective motion in the fluid caused by the moving interface (see Eq. (2.31) in [7]):

$$v_x = -\left(\frac{\rho_s}{\rho_\ell} - 1\right)\frac{dS}{dt} \tag{25}$$

Thus, when the plastic shrinks upon solidification, the melt moves towards the solidification front, where dS/dt is the speed of the solidification front.

The solution chosen for the solid region is:

$$\Theta_s = C_1 + C_2 \operatorname{erf}\left(\frac{x}{\sqrt{4\alpha_s t}}\right) \tag{26}$$

and, for the liquid:

$$\Theta_\ell = \left(C_3 + C_4\right) - C_4 \operatorname{erfc}\left(\frac{x}{\sqrt{4\alpha_\ell t}} + \frac{S(t)}{\sqrt{4\alpha_\ell t}}\frac{\rho_s - \rho_\ell}{\rho_\ell}\right) \tag{27}$$

where the boundary conditions are:

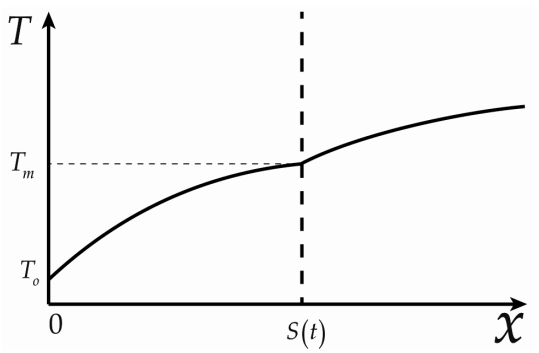

Fig. 15 One dimensional solidification in semi-infinite half space on isothermal wall

$$\Theta_s(0,t)=0 \tag{28}$$

$$\Theta_\ell(\infty,t)=1 \tag{29}$$

$$\Theta_\ell=\Theta_s=\Theta_m;x=S(t) \tag{30}$$

From Eq. (28), we get $C_1=0$ and, from Eq. (29), $C_3+C_4=1$. Next, we can set Eqs. (26) and (27) equal to $\Theta=\Theta_m$ at $x=S(t)$, and letting:

$$\lambda\equiv\frac{S(t)}{\sqrt{4\alpha_s t}} \tag{31}$$

we get:

$$C_2=\frac{\Theta_m}{\operatorname{erf}(\lambda)} \tag{32}$$

and

$$C_4=\frac{1-\Theta_m}{\operatorname{erfc}\left[\lambda\left(\frac{\alpha_s}{\alpha_\ell}\right)^{\frac{1}{2}}\left(\frac{\rho_s}{\rho_\ell}\right)\right]} \tag{33}$$

so that the temperature profiles in the liquid and solid region are:

$$\Theta_s=\frac{\Theta_m}{\operatorname{erf}(\lambda)}\operatorname{erf}\left(\frac{x}{\sqrt{4\alpha_s t}}\right) \tag{34}$$

and

$$\Theta_\ell=1-\frac{1-\Theta_m}{\operatorname{erfc}\left[\lambda\left(\frac{\alpha_s}{\alpha_\ell}\right)^{\frac{1}{2}}\left(\frac{\rho_s}{\rho_\ell}\right)\right]}\operatorname{erfc}\left(\frac{x}{\sqrt{4\alpha_\ell t}}+\frac{S(t)}{\sqrt{4\alpha_\ell t}}\frac{\rho_s-\rho_\ell}{\rho_\ell}\right) \tag{35}$$

Now, considering the heat flux boundary condition at the solidification front (including the term for the pressure jump [17-18]; see also Eq. (2.33d) in [7]):

$$k_s\left.\frac{\partial\Theta_s}{\partial x}\right|_{x=S(t)}-k_\ell\left.\frac{\partial\Theta_\ell}{\partial x}\right|_{x=S(t)}=\frac{\rho_s}{T_i-T_o}\frac{dS(t)}{dt}\left[\Delta\hat{H}_f-P\left(\frac{1}{\rho_\ell}-\frac{1}{\rho_s}\right)\right] \tag{36}$$

where:

$$\frac{\partial\Theta_s}{\partial x}=\frac{C_2}{\sqrt{\pi t\alpha_s}}\exp\left[-\left(\frac{x}{\sqrt{4\alpha_s t}}\right)^2\right] \tag{37}$$

and

$$\frac{d\Theta_\ell}{dx}=\frac{C_4}{\sqrt{\pi t\alpha_\ell}}\exp\left[-\left(\frac{x}{\sqrt{4\alpha_\ell t}}+\lambda\left(\frac{\alpha_s}{\alpha_\ell}\right)^{\frac{1}{2}}\frac{\rho_s-\rho_\ell}{\rho_\ell}\right)^2\right] \tag{38}$$

Substituting Eq. (32) into Eq. (37) and Eq. (33) into Eq. (38), and then these into Eq. (36) yields:

$$\frac{\exp(-\lambda^2)}{\operatorname{erf}(\lambda)}\Theta_m+\frac{k_\ell}{k_s}\left(\frac{\alpha_s}{\alpha_\ell}\right)^{\frac{1}{2}}\frac{\exp\left(-\lambda^2\left(\frac{\alpha_s}{\alpha_\ell}\right)\left(\frac{\rho_s}{\rho_\ell}\right)^2\right)}{\operatorname{erfc}\left[\lambda\left(\frac{\alpha_s}{\alpha_\ell}\right)^{\frac{1}{2}}\left(\frac{\rho_s}{\rho_\ell}\right)\right]}(\Theta_m-1)$$

$$=\frac{\lambda\sqrt{\pi}}{\hat{C}_{p,s}(T_i-T_o)}\left[\Delta\hat{H}_f-P\left(\frac{1}{\rho_\ell}-\frac{1}{\rho_s}\right)\right] \tag{39}$$

If we then neglect the pressure jump, Eq. (39) reduces to (see Eq. (2.42b) in [7]):

$$\frac{\exp(-\lambda^2)}{\operatorname{erf}(\lambda)}\Theta_m+\frac{k_\ell}{k_s}\left(\frac{\alpha_s}{\alpha_\ell}\right)^{\frac{1}{2}}\frac{\exp\left(-\lambda^2\left(\frac{\alpha_s}{\alpha_\ell}\right)\left(\frac{\rho_s}{\rho_\ell}\right)\right)}{\operatorname{erfc}\left[\lambda\left(\frac{\alpha_s}{\alpha_\ell}\right)^{\frac{1}{2}}\left(\frac{\rho_s}{\rho_\ell}\right)\right]}(\Theta_m-1)$$

$$=\mathbb{H}\lambda\sqrt{\pi} \tag{40}$$

and for the special case of constant density, Eq. (40) reduces to:

$$\frac{\Theta_m}{\operatorname{erf}(\lambda)}\exp(-\lambda^2)+\frac{\Theta_m-1}{\operatorname{erfc}\left(\lambda(\alpha_s/\alpha_\ell)^{\frac{1}{2}}\right)}\frac{k_\ell}{k_s}\left(\frac{\alpha_s}{\alpha_\ell}\right)^{\frac{1}{2}}\exp\left(-\lambda^2\frac{\alpha_s}{\alpha_\ell}\right)$$

$$=\mathbb{H}\lambda\sqrt{\pi} \tag{41}$$

which agrees well with experimental data (see Fig. 5 of [19]; see also Section 1.3.4.2 in [20-22]. When all the properties are constant, Eq. (41) reduces to:

$$\mathbb{H}=\frac{\exp(-\lambda^2)}{\lambda\sqrt{\pi}}\left(\frac{\Theta_m}{\operatorname{erf}\lambda}-\frac{1-\Theta_m}{\operatorname{erfc}\lambda}\right) \tag{42}$$

which is Eq. 12C.3-3 in [6], which we have plotted Eq. (42) in Fig. 12. We can also accurately approximate the transcendental function Eq. (42) with the explicit formula:

$$\lambda\cong\frac{1}{2}\left[\frac{1}{\sqrt{\pi}}\frac{\Theta_m}{\mathbb{H}}+\sqrt{\frac{2(1-\Theta_m)}{\mathbb{H}}+\frac{1}{\pi}\left(\frac{\Theta_m}{\mathbb{H}}\right)^2}\right];\lambda\le\frac{1}{10} \tag{43}$$

for small values of λ. In the absence of phase change, $\mathbb{H}=0$ and Eq. (42) reduces to:

$$\Theta_m=\operatorname{erf}\lambda_0 \tag{44}$$

We use λ_0 to define Λ in Table 3.